

# Analysis of $B_s \rightarrow KK$ decays in the PQCD

Chuan-Hung Chen

*Department of Physics, National Cheng Kung University  
Tainan, Taiwan, Republic of China*

## Abstract

We study  $B_s \rightarrow KK$  decays in the framework of the PQCD. We show that the branching ratios of  $B_s \rightarrow (K^+K^-, K^0\bar{K}^0)$  are about  $(22.43, 25.78) \times 10^{-6}$  for  $\phi_3(\gamma) \simeq 72^\circ$ , which are consistent with the model-independent estimations. We find that the typical scale of the decays is near 1.7 GeV. We also point out that the induced strong phase  $\delta$  is around  $207^\circ$  so that the direct CP asymmetry of  $B_s \rightarrow K^+K^-$  could reach 15%.

The study of charmless B decays has an enormous progress since many decays such as those with exclusive pseudoscalar-pseudoscalar final states ( $B \rightarrow PP$ ) were measured at  $e^+e^-$  machines by CLEO [1], BABAR [2] and Belle [3], respectively. From the search of B decays, we not only could test the origin of CP violation in standard model (SM), which is the consequence of the Cabibbo-Kobayashi-Maskawa (CKM) quark-mixing matrix [4] but also verify various QCD approaches for nonperturbative problems in exclusive decays. Recently, the proposals of using the mixing-induced and direct CP asymmetries in  $B_d \rightarrow \pi^+\pi^-$  and  $B_s \rightarrow K^+K^-$  [5] or the branching ratios (BRs) of  $B_s \rightarrow K^+K^-$  and  $K^0\bar{K}^0$  decays [6] are suggested to determine the angle  $\phi_3$  or  $\gamma$ . Clearly, it is important to give a detailed analysis on the decays of  $B_s \rightarrow KK$ .

It is known that one of the main theoretical uncertainties for studying exclusive hadron decays is from the calculations of matrix elements. Usually it is performed in the perturbative QCD (PQCD) approach developed by Brodsky and Lepage (BL) [7]. In the BL formalism, the nonperturbative part is included in the hadron wave functions and the transition amplitude is factorized into the convolution of hadron wave functions and the hard amplitude of the valence quarks. However, with the BL approach, it has been pointed out that perturbative evaluation of the pion form factor suffers a non-perturbative enhancement from the end-point region with a momentum fraction  $x \rightarrow 0$  [8]. If so, the hard amplitude is characterized by a low scale, such that the expansion in terms of a large coupling constant  $\alpha_s$  is not reliable. Furthermore, more serious end-point (logarithmic) singularities are observed in the twist-2 (leading-twist) contribution to the  $B \rightarrow \pi$  transition form factors [9, 10]. The singularities even become linear while including the twist-3 (next-to-leading twist) wave function [11]. Because of these singularities, it was claimed that form factors are dominated by the soft dynamics and not calculable in the PQCD [12].

In order to take care of the end-point singularities,  $k_T$ , the transverse momentum of the valence-quark [13], and threshold resummations [14, 15] have to be introduced. The inclusion of  $k_T$  will bring in large double logarithms  $\alpha_s \ln^2(k_T/M_B)$  through radiative corrections. Therefore, these large logarithms should be resummed in order to improve the perturbative calculation. Due to the resummation [13, 16, 17], the arisen distribution of  $k_T$  exhibits a suppression in the region with  $k_T \sim O(\bar{\Lambda})$  [19] and the average of  $k_T^2$  is enlarged up to around  $\langle k_T^2 \rangle \sim \bar{\Lambda}M_B$  for  $M_B \sim 5$  GeV; consequently, the off-shellness of internal particles keeps being  $O(\bar{\Lambda}M_B)$  even in the end-point region. Moreover, due to the radiative corrections of the weak vertex [18], another type of double logarithms  $\alpha_s \ln^2 x$  actually exists while  $x \rightarrow 0$ ; and therefore, these large corrections should be also resummed, called threshold resummation [14, 15], for justifying the perturbative expansion so that the result leads to a strong Sudakov suppression at  $x \rightarrow 0$ . Hence, including  $k_T$  and threshold resummations, the end-point singularities can be dealt with self-consistent in the PQCD.

In the literature, the applications of the modified PQCD (MPQCD) [22] to the processes of  $B \rightarrow PP$ , such as  $B \rightarrow K\pi$  [21],  $B \rightarrow \pi\pi$  [23],  $B \rightarrow KK$  [24] and  $B \rightarrow K\eta^{(\prime)}$  [25], as well as that of  $B \rightarrow VP$  such as  $B \rightarrow \phi\pi$  [26],  $B \rightarrow \rho(\omega)\pi$  [27] and  $B \rightarrow \phi K$  [28, 29] have been studied and found that they are consistent with the experimental data or limits. For a review on the PQCD approach, we summary the characters of the MPQCD briefly as follows:

- Due to the introduction of  $k_T$  and threshold resummations for smearing the singularities, the  $B \rightarrow \pi, K$  form factors are still dominated in the perturbative region with  $\alpha_s/\pi < 0.2$  [21].

- There involve three scales in the MPQCD: the  $M_W$  scale of the electroweak (EW) interaction, the typical scale  $t$  which reflects the specific dynamics of the heavy meson decays, and the factorization scale of  $\Lambda \simeq M_B - M_b$  with  $M_B$  and  $M_b$  being the B-meson and b-quark masses, which shows the interface of the soft and hard QCD dynamics, respectively. We note that the  $t$  scale is chosen such that the contributions from higher order effects are as small as possible [20] and one can find the specific scale to be the chiral symmetry breaking scale [21, 29].
- Penguin enhancement: As known, Wilson coefficients (WCs) of  $C_4(\mu)$  and  $C_6(\mu)$  generated from the QCD penguin [32] increase significantly at  $t < M_B/2$ . Due to the enhancements, it is realized that the BRs of  $B \rightarrow \phi K$  in the MPQCD [28, 29] can explain the results of Belle [30] and BaBar [31] naturally.
- Less theoretical uncertainties: The main theoretical uncertainties in the MPQCD from are the shape parameter  $\omega_B$  of the B-meson wave function, chiral symmetrical breaking parameter  $m_P^0$  introduced by the matrix element of the pseudoscalar nonlocal operator for the  $P$  meson [19, 33], and the power factor  $c$  for the parametrization of the Sudakov factor  $S_t \propto [x(1-x)]^c$  generated by the threshold resummation, respectively. With experiments, one would precisely set the limits on these theoretical unknown parameters.
- Large absorptive parts: The major absorptive parts arise from the annihilation topology in which the propagator of the internal quark satisfies the on-shell condition. With the power counting rule, the ratios of the transition form factor ( $F^{BK}$ ) to the imaginary and real parts of annihilation contributions are found to be  $F^{BK} : ImF^{KK} : ReF^{KK} = 1 : 2m_K^0/M_B : \Lambda/M_B$  [29]. For  $M_B \sim 5.0$  GeV, the value of the imaginary part is compatible with that of the form factor.

In this paper, to calculate the matrix elements of four-quark operators relevant to the  $B_s \rightarrow KK$  decays, we adopt the MPQCD factorization formalism as

$$\begin{aligned}
\langle VK | \mathcal{O}_k | B \rangle &= \int [dx] \int \left[ \frac{d^2 \vec{b}}{4\pi} \right] \Phi_K^*(x_3, \vec{b}_3) \Phi_K^*(x_2, \vec{b}_2) \\
&\times T_k(\{x\}, \{\vec{b}\}, M_B) \Phi_{B_s}(x_1, \vec{b}_1) \\
&\times S_t(\{x\}) e^{-S(\{x\}, \{\vec{b}\}, M_B)}
\end{aligned} \tag{1}$$

where  $\Phi_K^*$  and  $\Phi_{B_s}$  are the wave functions of  $K$  and  $B_s$ ,  $T_k$  is the hard scattering amplitude dictated by  $\mathcal{O}_k$  operators, the exponential factor is the Sudakov factor [16, 17], and  $S_t(x)$  [18, 19] expresses the threshold resummation factor. Since  $B_s$  is a heavy meson, the chiral symmetry breaking effects are negligible so that  $\Phi_{B_s}$  is regarded as  $\Phi_{B_{d,u}}$ .

The effective Hamiltonian for decays with the  $b \rightarrow s$  transition is given by

$$H_{\text{eff}} = \frac{G_F}{\sqrt{2}} \sum_{q'=u,c} V_{q's} \left[ C_1(\mu) \mathcal{O}_1^{(q')} + C_2(\mu) \mathcal{O}_2^{(q')} + \sum_{i=3}^{10} C_i(\mu) \mathcal{O}_i \right] \tag{2}$$

where  $V_{q'} = V_{q's}^* V_{q'b}$  are the products of the CKM matrix elements,  $C_i(\mu)$  are the WCs and  $\mathcal{O}_i$  correspond to four-quark operators, and their detailed expressions can be found in

Ref.[32]. It is easy to find that the structures of  $\mathcal{O}_{3,4,5,6}$ , generated by the QCD penguin, are the same as that of  $\mathcal{O}_{9,10,7,8}$  from the EW penguin, respectively. Except the different color flows between  $O_{2i-1}$  and  $O_{2i}$  ( $i = 1, 2, \dots, 5$ ), each of the pair operators also has the same structure. Therefore, we can define the useful EW dynamical variables as

$$\begin{aligned}
a_1 &= C_1 + \frac{C_2}{N_c}, & a_2 &= C_2 + \frac{C_1}{N_c}, & a'_{1,2} &= \frac{C_{2,1}}{N_c}, \\
a_{3,4}^q &= C_{3,4} + \frac{3e_q}{2}C_{9,10} + a_{3,4}^{\prime q}, & a_{3,4}^{\prime q} &= \frac{C_{4,3}}{N_c} + \frac{3e_q}{2N_c}C_{10,9}, \\
a_{5,6}^q &= C_{5,6} + \frac{3e_q}{2}C_{7,8} + a_{5,6}^{\prime q}, & a_{5,6}^{\prime q} &= \frac{C_{6,5}}{N_c} + \frac{3e_q}{2N_c}C_{8,7},
\end{aligned} \tag{3}$$

where the superscript  $q$  can be the light u, d and s quarks, respectively. We note that all decay amplitudes related to the weak dynamical interactions are dependent on  $a_j^{(q)}$  and  $a_j^{\prime(q)}$  ( $j = 1, 2, \dots, 6$ ), while nonfactorizable effects are only associated with the color suppressed variables  $a_j^{\prime(q)}$ .

By defining the decay rates as

$$\Gamma = \frac{G_F^2 M_B^3}{32\pi} |\mathcal{A}|^2$$

with  $G_F$  and  $M_B$  being the Fermi constant and the mass of  $B_s$ , the corresponding decay amplitudes for  $B_s \rightarrow K^+ K^-$  and  $B_s \rightarrow K^0 \bar{K}^0$  modes are written by

$$\begin{aligned}
\mathcal{A}^{+-} &= f_K V_t^* F_{e46}^{P(u)} + V_t^* \mathcal{M}_{e46}^{P(u)} + f_B V_t^* F_{a6}^{P(s)} + V_t^* (\mathcal{M}_{a46}^{P(s)} + \mathcal{M}_{a35}^{P(s)} + \mathcal{M}_{a35}^{P(u)}) \\
&\quad - f_K V_u^* F_{e2} - V_u^* \mathcal{M}_{e2} - V_u^* \mathcal{M}_{a1}, \\
\mathcal{A}^{00} &= f_K V_t^* F_{e46}^{P(d)} + V_t^* \mathcal{M}_{e46}^{P(d)} + f_B V_t^* F_{a6}^{P(s)} + V_t^* (\mathcal{M}_{a46}^{P(s)} + \mathcal{M}_{a35}^{P(s)} + \mathcal{M}_{a35}^{P(d)}),
\end{aligned} \tag{4}$$

respectively, where  $f_{K(B)}$  is the  $K(B)$  decay constant. In Eq. (4),  $\{F_{e(a)}^{[P(q)]}\}$  denote the factorizable emission (annihilation) transition form factors for tree [penguin] diagram contributions, while  $\{\mathcal{M}_{e(a)}^{[P(q)]}\}$  correspond to nonfactorizable effects, the superscript  $q$  represents the  $q$  quark pair emitted from the EW penguins, the subscripts of 1-6 label the WCs of Eq. (3) appearing in the factorization formulas, and the nonfactorizable amplitudes  $\mathcal{M}_{e2(a1)}$  are from the operators  $O_{1,2}^{(u)}$ . Note that there is no tree contribution to the decay of  $B_s \rightarrow K^0 \bar{K}^0$ . Explicitly, one has that

$$\begin{aligned}
F_{e46}^{P(q)} &= F_4^{P(q)} + F_6^{P(q)}, \\
F_4^{P(q)} &= 8\pi C_F M_B^2 \int_0^1 dx_1 dx_2 \int_0^\infty b_1 db_1 b_2 db_2 \phi_B(x_1, b_1) \\
&\quad \times \{[(1+x_2)\phi_K(1-x_2) + r_K(1-2x_2)(\phi_K^p(x_2) + \phi_K^s(x_2))] \\
&\quad \times E_{e4}^{(q)}(t_e^{(1)})h_e(x_1, x_2, b_1, b_2) \\
&\quad + 2r_K \phi_K^p(x_2) E_{e4}^{(q)}(t_e^{(2)})h_e(x_2, x_1, b_2, b_1)\},
\end{aligned} \tag{5}$$

$$\begin{aligned}
F_6^{P(q)} &= 16\pi C_F M_B^2 r_K \int_0^1 dx_1 dx_2 \int_0^\infty b_1 db_1 b_2 db_2 \phi_B(x_1, b_1) \\
&\quad \times \{[\phi_K(1-x_2) + r_K((2+x_2)\phi_K^p(x_2) - x_2\phi_K^s(x_2))] \\
&\quad \times E_{e6}^{(q)}(t_e^{(1)})h_e(x_1, x_2, b_1, b_2) \\
&\quad + [2r_K \phi_K^p(x_2)] E_{e6}^{(q)}(t_e^{(2)})h_e(x_2, x_1, b_2, b_1)\},
\end{aligned} \tag{6}$$

$$\begin{aligned}
F_{a6}^{P(s)} &= 16\pi C_F M_B^2 r_K \int_0^1 dx_2 dx_3 \int_0^\infty b_2 db_2 b_3 db_3 \\
&\times \{ [2\phi_K^p(x_2)\phi_K(x_3) + x_3\phi_K(x_2)(\phi_K^p(x_3) - \phi_K^s(x_3))] \\
&\times E_{a6}^{(s)}(t_a^{(1)})h_a(x_2, x_3, b_2, b_3) \\
&+ [2\phi_K(x_2)\phi_K^p(x_3) + x_2\phi_K(x_3)(\phi_K^p(x_2) - \phi_K^s(x_2))] \\
&\times E_{a6}^{(s)}(t_a^{(2)})h_a(x_3, x_2, b_3, b_2) \} , \tag{7}
\end{aligned}$$

with  $r_K = m_K^0/M_B$  for  $q = u$ - or  $d$ -quark. Here,  $C_F = 4/3$  is the color factor,  $\phi_B$  and  $\phi_K$  belong to twist-2  $B_s$  and  $K$  wave functions, while  $\phi_K^p$  and  $\phi_K^s$  are for twist-3 [33] and their detailed expressions can be found in Ref. [29], the hard part functions  $h_{e(a)}$  have included the  $S_i$  factor [29] and the evolution factors are given by

$$E_{ei}^{(q)}(t) = \alpha_s(t)a_i^{(q)}(t) \exp[-S_B(t, x_1) - S_K(t, x_2)] , \tag{8}$$

$$E_{ai}^{(q)}(t) = \alpha_s(t)a_i^{(q)}(t) \exp[-S_K(t, x_2) - S_K(t, x_3)] , \tag{9}$$

respectively. As expected that the nonfactorizable effects are smaller and more complicated, we do not display their expressions here but they will be included in the numerical calculations. We note that in our PQCD approach the  $x$  dependence in the kaon wave function is usually assigned to the momentum fraction of the light  $u$  or  $d$  quark [29]. However, due to the  $s$  quark being spectator in emission contributions, for simplified the hard parts, we adopt that this  $s$  quark carries a momentum fraction of  $x$  so that in order to compensate this change, the arguments  $x_2$  of the kaon wave functions  $\{\phi_K(x_2)\}$  in Eqs. (5) and (6) are replaced by  $1 - x_2$  in which we also have used the properties of  $\phi_K^p(1 - x_2) = \phi_K^p(x_2)$  and  $\phi_K^s(1 - x_2) = -\phi_K^s(x_2)$  [33, 29]. On the other hand, the factorizable annihilation contribution, associated with WC  $a_4^{(q)}$  and described by

$$\begin{aligned}
F_{a4}^{P(q)} &= 16\pi C_F M_B^2 \int_0^1 dx_2 dx_3 \int_0^\infty b_2 db_2 b_3 db_3 \\
&\times \left\{ \left[ x_3\phi_K(x_2)\phi_K(x_3) + 2r_K^2\phi_K^p(x_2)((1+x_3)\phi_K^p(x_3) \right. \right. \\
&\quad \left. \left. - (1-x_3)\phi_K^s(x_3)) \right] E_{a4}^{(q)}(t_a^{(1)})h_a(x_2, x_3, b_2, b_3) \right. \\
&\quad \left. - \left[ x_2\phi_K(x_2)\phi_K(x_3) + 2r_K^2\phi_K^p(x_3)((1+x_2)\phi_K^p(x_2) \right. \right. \\
&\quad \left. \left. - (1-x_2)\phi_K^s(x_2)) \right] E_{a4}^{(q)}(t_a^{(2)})h_a(x_3, x_2, b_3, b_2) \right\} , \tag{10}
\end{aligned}$$

vanishes. It can be seen easily by interchanging the integration variables  $x_2$  and  $x_3$  in the second terms of Eq.(10). However, this property does not apply to the annihilation contributions associated with  $a_6^{(q)}$  which are constructive in Eq. (7). The factorization formulas for  $F_{a1}$  and  $F_{a35}^{P(q)}$ , associated with the WCs of  $a_1(t_a)$  and  $a_3^{(q)}(t_a) + a_5^{(q)}(t_a)$ , are the same as  $F_{a4}^{P(s)}$ , *i.e.*, vanish.

In the numerical analysis, we first show the  $B_s \rightarrow K$  form factor of  $F^{B_s K}$  in Figure 1, which can be easily obtained by dropping the WC dependence out of Eq. (5), where we have used  $f_B = 0.20$  and  $f_K = 0.16$  GeV. For a comparison, we also display the results of  $B_d \rightarrow K$  form factor ( $F^{B_d K}$ ) from  $\{\phi_K(x_2)\}$  and  $M_{B_d}$  instead of  $\{\phi_K(1 - x_2)\}$  and  $M_{B_s}$ , respectively. From the figure, we see that  $F^{B_s K}$  is slightly less than  $F^{B_d K}$  and the main difference is from the chiral symmetry breaking effect appearing in  $\phi_K$  arisen from the different argument of  $\phi_K$ . After including WCs, the values of individual terms in Eq. (4) can be read from Table 1.

Table 1: The values of individual transition form factors (TFFs) for  $B_s \rightarrow KK$  decays with  $\omega_B = 0.4$ , two sets of  $m_K^0$  and  $\mathcal{M}_{aP}^{P(q)} = \mathcal{M}_{a35}^{P(q)} + \mathcal{M}_{a35}^{P(s)} + \mathcal{M}_{a46}^{P(s)}$ .

TFF	$F_{e46}^{P(u)}$	$F_{e46}^{P(d)}$	$F_{a6}^{P(s)}$	$F_{e2}$	$\mathcal{M}_{e46}^{P(u)}$
$m_K^0 = 1.7$	-31.91	-32.67	$-1.25 + i10.91$	369.37	$0.17 + i0.32$
$m_K^0 = 1.5$	-27.00	-27.64	$-1.10 + i9.63$	336.53	$0.16 + i0.28$
TFF	$\mathcal{M}_{e46}^{P(d)}$	$\mathcal{M}_{aP}^{P(u)}$	$\mathcal{M}_{aP}^{P(d)}$	$\mathcal{M}_{e2}$	$\mathcal{M}_{a1}$
$m_K^0 = 1.7$	$0.16 + i0.48$	$0.19 + i0.52$	$0.20 + i0.54$	$-1.19 - i2.75$	$0.69 - i4.3$
$m_K^0 = 1.5$	$0.16 + i0.45$	$0.15 + i0.50$	$0.15 + i0.52$	$-1.36 - i2.95$	$0.59 - i4.04$

The slight difference between  $F_{e46}^{P(u)}$  and  $F_{e46}^{P(d)}$  comes from the EW effects. The factorizable annihilation and nonfactorizable contributions are complex because the on-shell condition can only be satisfied in these diagrams. On the other hand, in order to know the strong phase more clearly, we reparametrize the decay amplitudes as

$$A = V_t^* P - V_u^* T = -V_c^* P \left( 1 + \left| \frac{V_u}{V_c} \right| r e^{i(\delta+\phi_3)} \right) \quad (11)$$

with  $r e^{i\delta} = 1 + T/P$ , where we have used  $\sum_{i=\{u,c,t\}} V_i = 0$ ,  $T$  and  $P$  express the whole tree and penguin contributions,  $\delta$  describes the strong phase, and the values of  $r$  and  $\delta$  are shown in Table 2. From the table, we clearly see that  $\cos\delta < 0$  in the MPQCD approach.

Table 2: The results of  $r$  and  $\delta$  with different values of  $\omega_B$  and  $m_K^0$ .

$m_K^0$	1.7		1.6		1.5	
$\omega_B$	$r$	$\delta(\text{deg})$	$r$	$\delta(\text{deg})$	$r$	$\delta(\text{deg})$
0.41	9.16	207.7	9.42	208.0	9.70	208.3
0.40	9.22	206.9	9.49	207.2	9.78	207.6
0.38	9.34	205.3	9.63	205.6	9.92	205.9

To calculate the CP average BRs of  $B_s \rightarrow KK$  decays, we use the following data as input values:

$$V_{us} \approx \lambda, \quad V_{ts} \approx -A\lambda^2, \quad V_{ub} \approx A\lambda^3 R_b e^{-i\phi_3}, \quad A \approx 0.80, \quad \lambda \approx 0.22, \quad R_b \approx 0.36.$$

From these values, the results with possible  $\omega_B$  and  $m_K^0$  are displayed in Table 3. We note that although the transition form factor of the tree contribution is larger than others by over one order of the magnitude as shown in Table 1, due to the suppression of CKM matrix elements, actually the tree contribution is subdominant. By fixing WCs at some specific scales, the results are given in Figure 2. From that, we clearly see that the typical scale for the  $B_s \rightarrow KK$  decays is around 1.7 GeV. In Figure 3, we also show the BR of  $B_s \rightarrow K^+ K^-$  as a function of angle  $\phi_3$ .

As usual, the direct CP asymmetry (CPA) can be defined as

$$A_{CP} = \frac{\Gamma(B_s \rightarrow K^+ K^-) - \Gamma(\bar{B}_s \rightarrow K^- K^+)}{\Gamma(B_s \rightarrow K^+ K^-) + \Gamma(\bar{B}_s \rightarrow K^- K^+)},$$

Table 3: The BRs (in units of  $10^{-6}$ ) of  $B_s \rightarrow KK$  decays with different values of  $\omega_B$  and  $m_K^0$ .

$Br$	$B_s \rightarrow K^+K^-$			$B_s \rightarrow K^0\bar{K}^0$		
	$m_K^0 = 1.7$	$m_K^0 = 1.6$	$m_K^0 = 1.5$	$m_K^0 = 1.7$	$m_K^0 = 1.6$	$m_K^0 = 1.5$
$\omega_B = 0.41$	21.08	18.18	15.58	24.22	20.96	18.04
$\omega_B = 0.40$	22.43	19.33	16.55	25.78	22.32	19.20
$\omega_B = 0.38$	25.56	21.97	18.77	29.50	25.45	21.84

$$= -\frac{2\lambda^2 R_b r \sin\delta \sin\phi_3}{(1 + (\lambda^2 R_b r)^2 + 2\lambda^2 R_b r \cos\delta \cos\phi_3)} \quad (12)$$

by using Eq. (11). From Eq. (12), we see that the CPA is associated with both weak CP and strong phases. The results as a function of angle  $\phi_3$  are plotted in Figure 4.

In the following, we present the implications of our results. With the limit of SU(3) symmetry, it is known that  $\Gamma(B_d \rightarrow K^+\pi^-) \approx \Gamma(B_s \rightarrow K^+K^-)$  and  $\Gamma(B_d \rightarrow K^0\bar{K}^0) \approx |V_{td}/V_{ts}|^2 \Gamma(B_s \rightarrow K^+K^-)$  [34]. With including SU(3) breaking effects, one has [6]

$$Br(B_s \rightarrow K^\pm K^\mp) \approx \frac{\tau_{B_s}}{\tau_{B_d}} \left(\frac{M_{B_s}}{M_{B_d}}\right)^3 \left(\frac{F^{B_s K}(0)}{F^{B_d \pi}(0)}\right)^2 Br(B_d \rightarrow K^\pm \pi^\mp), \quad (13)$$

$$Br(B_s \rightarrow K^0 \bar{K}^0) \approx \frac{\tau_{B_s}}{\tau_{B_d}} \left(\frac{M_{B_s}}{M_{B_d}}\right)^3 \left|\frac{V_{ts} F^{B_s K}(0)}{V_{td} F^{B_d K}(0)}\right|^2 Br(B_d \rightarrow K^0 \bar{K}^0). \quad (14)$$

We note that  $Br(B_d \rightarrow K^\pm \pi^\mp)$  has been observed in the present B factories [2, 3, 35] and although there is no limit on  $Br(B_d \rightarrow K^0 \bar{K}^0)$ , its estimation has been done by the PQCD in Ref. [24]. By taking  $Br(B_d \rightarrow K^\pm \pi^\mp) \simeq 18.5 \times 10^{-6}$  and  $Br(B_d \rightarrow K^0 \bar{K}^0) \simeq 1.4 \times 10^{-6}$ , we get  $Br(B_s \rightarrow K^\pm K^\mp) \simeq 22.68 \times 10^{-6}$  and  $Br(B_s \rightarrow K^0 \bar{K}^0) \simeq 26.05 \times 10^{-6}$ . Comparing with the values in Table 3, obviously the results are consistent with the those from the MPQCD for  $\omega_B = 0.4$ ,  $m_K^0 = 1.7$  GeV and  $\phi_3 \simeq 72^\circ$ . If so, the MPQCD prefers  $\phi_3$  to be less than  $90^\circ$ . On the other hand, if neglecting the small difference from EW effects ( $\sim 7\%$  difference in our analysis), from Eq. (11), we find that [6]

$$Br(B_s \rightarrow K^\pm K^\mp) \approx Br(B_s \rightarrow K^0 \bar{K}^0) (1 + 2\lambda^2 R_b r \cos\delta \cos\phi_3). \quad (15)$$

In Eq. (15), if the interference term associated with  $\cos\phi_3 \cos\delta$  is negative, it gives  $Br(B_s \rightarrow K^\pm K^\mp) < Br(B_s \rightarrow K^0 \bar{K}^0)$ . In the MPQCD, it also implies that  $\phi_3 < 90^\circ$ . From Eq. (13), we also expect that  $A_{CP}(B_s \rightarrow K^\pm K^\mp) \approx A_{CP}(B_d \rightarrow K^\pm \pi^\mp)$ . Hence, by the measurements of  $B_s \rightarrow KK$  decays, the sign of  $\cos\phi_3 \cos\delta$  can be determined and the predictions of the MPQCD can also be verified.

Finally, we give a brief remark on the relations between  $B_s \rightarrow K^\pm K^\mp$  and  $B_d \rightarrow \pi^\pm \pi^\mp$  decays. It is known that, as shown in Ref. [5], there are close relationships for transition form factors between the decays by interchange of  $d$  and  $s$  quarks, called the U-spin transformation. Under the U-spin limit, both decays approximately have the same  $r$  and  $\delta$  as defined in Eq. (11). Moreover, we find that the term associated with  $\cos\delta \cos\phi_3$  in the  $B_d \rightarrow \pi^\pm \pi^\mp$  decay has an opposite sign to that in  $B_s \rightarrow K^\pm K^\mp$ . This implies that while one

of both distributions increases with respect to  $\phi_3$ , the other one will decrease [6]. Hence, by precise measurements on the BRs of  $B_d \rightarrow \pi^\pm \pi^\mp$  and  $B_s \rightarrow K^\pm K^\mp$ , we also can obtain the information of  $\cos \delta \cos \phi_3$ .

In summary, we have studied the  $B_s \rightarrow KK$  decays with the MPQCD approach. We have verified that the typical scale in the MPQCD is around 1.7 GeV and the large absorptive parts make  $\sin \delta \sim -0.45$  so that the CP asymmetry could be as large as 15%. Since the Tevatron Run II has started a new physics run at  $\sqrt{s} = 2$  TeV and will collect a data sample of  $2 \text{ fb}^{-1}$  in the first two years [36]. At its initial phase with 10K of  $B_s \rightarrow KK$  events, the BRs and CP asymmetry predicted by the MPQCD can be tested.

### Acknowledgments

The author would like to thank C. Q. Geng, Y.Y. Keum and H.N. Li for their useful discussions. This work was supported in part by the National Science Council of the Republic of China under contract numbers NSC-89-2112-M-006-033 and the National Center for Theoretical Science.



## References

- [1] CLEO Collaboration, T. Bergfeld *et al.*, Phys. Rev. Lett. **81**, 272 (1998).
- [2] BABAR Collaboration, B. Aubert *et al.*, hep-ex/0105061.
- [3] Belle Collaboration, K. Abe *et al.*, hep-ex/0104030.
- [4] M. Kobayashi and T. Maskawa, Prog. Theor. Phys. **49**, 652 (1973).
- [5] R. Fleischer, Phys. Lett. **B459**, 306 (1999).
- [6] C.H. Chen and C.Q. Geng, hep-ph/0107145.
- [7] G.P. Lepage and S.J. Brodsky, Phys. Lett. **B87**, 359 (1979); Phys. Rev. **D22**, 2157 (1980).
- [8] N. Isgur and C.H. Llewellyn-Smith, Nucl. Phys. **B317**, 526 (1989).
- [9] A. Szczepaniak, E. M. Henley, and S. Brodsky, Phys. Lett. **B243**, 287 (1990).
- [10] R. Akhoury, G. Sterman and Y.P. Yao, Phys. Rev. **D50**, 358 (1994).
- [11] M. Beneke and T. Feldmann, Nucl. Phys. **B592**, 3 (2000).
- [12] A. Khodjamirian and R. Ruckl, Phys. Rev. **D58**, 054013 (1998).
- [13] H.N. Li and G. Sterman, Nucl. Phys. **B381**, 129 (1992).
- [14] G. Sterman, Phys. Lett. **B179**, 281 (1986); Nucl. Phys. **B281**, 310 (1987).
- [15] S. Catani and L. Trentadue, Nucl. Phys. **B327**, 323 (1989); Nucl. Phys. **B353**, 183 (1991).
- [16] J.C. Collins and D.E. Soper, Nucl. Phys. **B193**, 381 (1981).
- [17] J. Botts and G. Sterman, Nucl. Phys. **B325**, 62 (1989).
- [18] H.N. Li, hep-ph/0102013.
- [19] T. Kurimoto, H.N. Li, and A.I. Sanda, hep-ph/0105003, to appear in PRD.
- [20] B. Melić, B. Nžić and K. Passek, Phys. Rev. **D60**, 074004 (1999).
- [21] Y.Y. Keum, H.N. Li, and A.I. Sanda, Phys. Lett. **B504**, 6 (2001); Phys. Rev. **D63**, 054008 (2001).
- [22] H.N. Li, Phys. Rev. **D64**, 014019 (2001).
- [23] C.D. Lü, K. Ukai, and M.Z. Yang, Phys. Rev. **D63**, 074009 (2001).
- [24] C.H. Chen and H.N. Li, Phys. Rev. **D63**, 014003 (2001).
- [25] E. Kou and A.I. Sanda, hep-ph/0106159.

- [26] B. Melic, Phys. Rev. D**59**, 074005 (1999).
- [27] C.D. Lü and MZ. Yang, hep-ph/0011238.
- [28] S. Mishima, hep-ph/0107163.
- [29] C.H. Chen, Y.Y. Keum and H.N. Li, hep-ph/0107165, to appear in PRD.
- [30] Belle Collaboration, A. Bozek, talk presented at the 4th International Workshop on B Physics and CP Violation, Ise-Shima, Japan, Feb. 19-23, 2001.
- [31] BaBar Collaboration, G. Cavoto, talk presented at the XXXVI Rencontres de Moriond, March 17-24, 2001.
- [32] G. Buchalla, A.J. Buras and M.E. Lautenbacher, Rev. Mod. Phys. **68**, 1230(1996).
- [33] P. Ball, JHEP **01**, 010 (1999).
- [34] M. Gronau, O.F. Hernández, D. London and J.L. Rosner, Phys. Rev. D**50**, 4529 (1994); *ibid.* **52**, 6356 (1995).
- [35] CLEO Collaboration, D. Cronin-Hennessy, Phys. Rev. Lett. **85**, 515 (2000).
- [36] CDF Collaboration, M. Tanaka, 7th International Conference on B-Physics at Hadron Machines, Sea of Galilee, Kibbutz Maagan, Israel, September 13-18, 2000.

## Figure Captions

- Figure 1: Form factors of (a)  $B_d \rightarrow K$  and (b)  $B_s \rightarrow K$  with respect to  $m_K^0$ . The dashed, solid and dashed-dot lines correspond to  $\omega_B = 0.38, 0.4$  and  $0.41$  GeV, respectively.
- Figure 2: BRs (in units of  $10^{-6}$ ) of (a)  $B_s \rightarrow K^0 \bar{K}^0$  and (b)  $B_s \rightarrow K^+ K^-$  with fixing the typical scale on WCs. The dashed, dashed-dot, dotted and dense-dot lines stand for  $t = 1.5, 1.7, 2.5, 4.8$  GeV, with  $\omega_B = 0.4$  GeV and  $\phi_3 = 72^\circ$  while the solid line is the result of  $t$  as a running scale, respectively.
- Figure 3: The CP average BR of  $B_s \rightarrow K^+ K^-$  as a function of  $\phi_3$  with  $\omega_B = 0.4$  GeV. The solid, dashed and dashed-dot lines denote  $m_K^0 = 1.7, 1.6$  and  $1.5$  GeV, respectively.
- Figure 4: The CP asymmetry of  $B_s \rightarrow K^+ K^-$  with  $m_K^0 = 1.7$  GeV. The dashed, solid and dashed-dot lines represent  $\omega_B = 0.41, 0.4$  and  $0.38$  GeV, respectively.

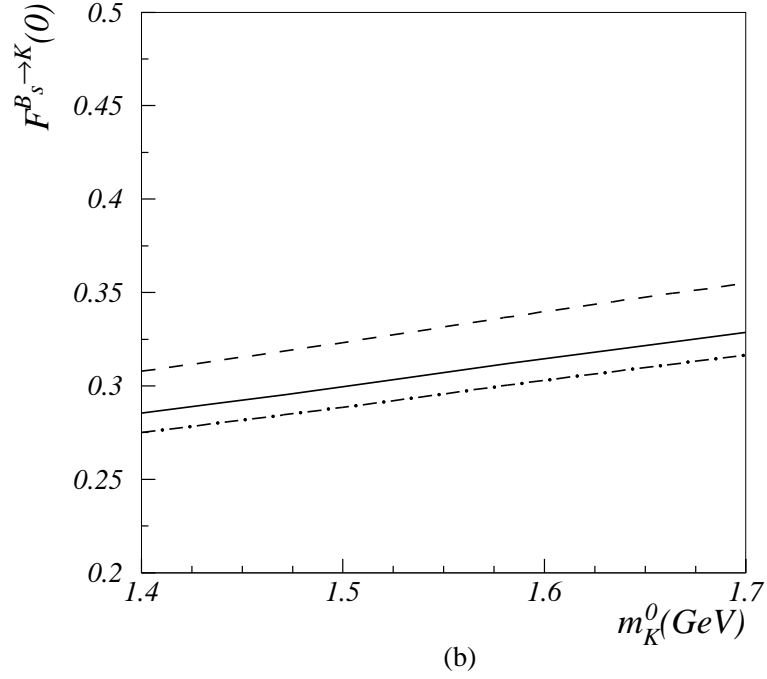
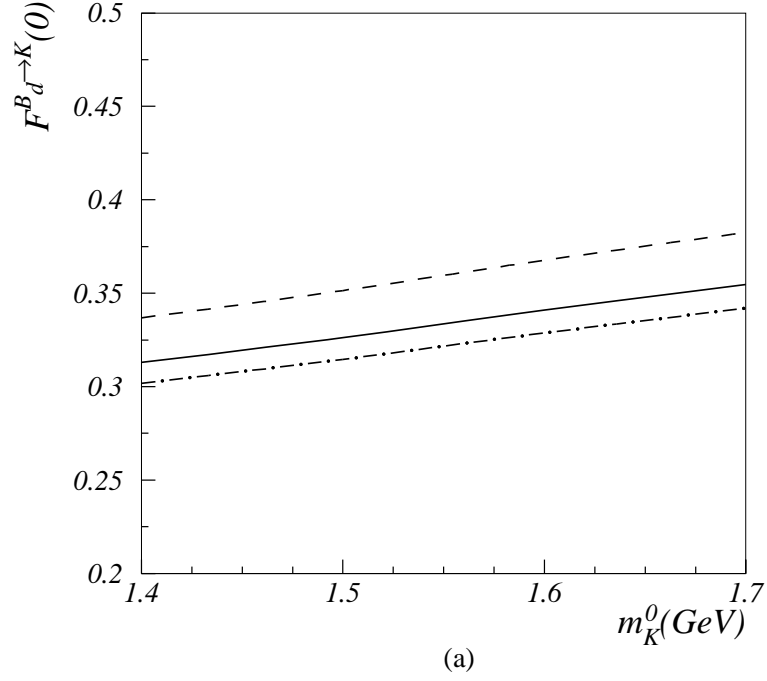


Figure 1: Form factors of (a)  $B_d \rightarrow K$  and (b)  $B_s \rightarrow K$  with respect to  $m_K^0$ . The dashed, solid and dashed-dot lines correspond to  $\omega_B = 0.38, 0.4$  and  $0.41$  GeV, respectively.

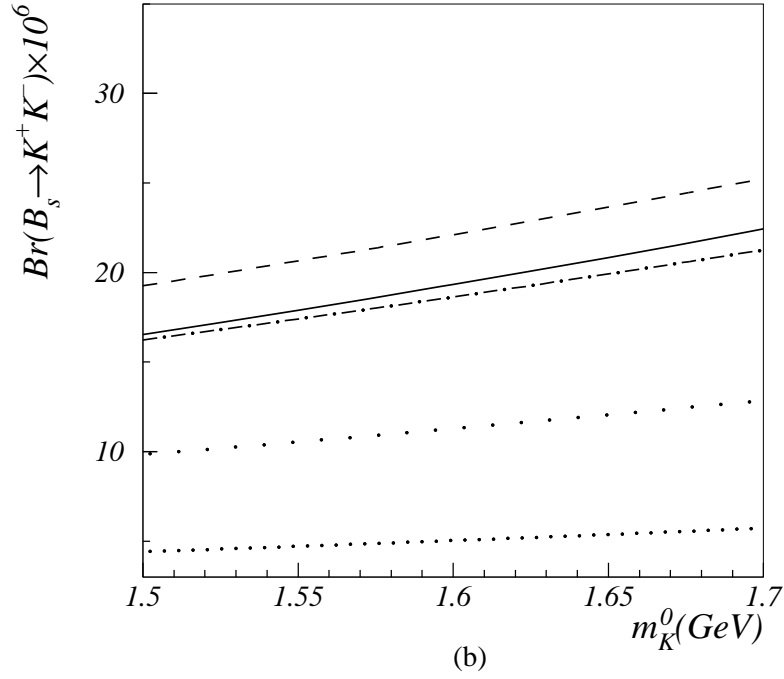
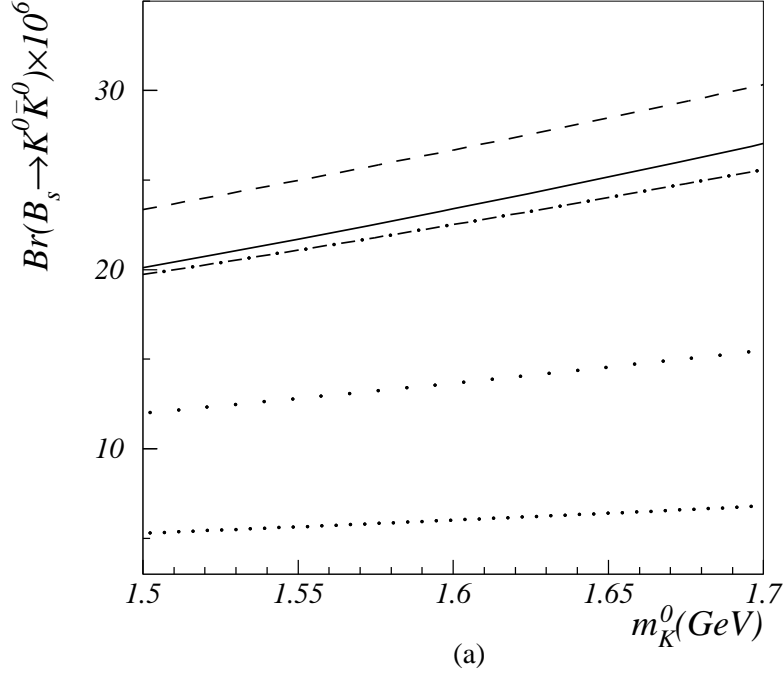


Figure 2: BRs (in units of  $10^{-6}$ ) of (a)  $B_s \rightarrow K^0 \bar{K}^0$  and (b)  $B_s \rightarrow K^+ K^-$  with fixing the typical scale on WCs. The dashed, dashed-dot, dotted and dense-dot lines stand for  $t=1.5, 1.7, 2.5, 4.8$  GeV, with  $\omega_B = 0.4$  GeV and  $\phi_3 = 72^\circ$  while the solid line is the result of  $t$  as a running scale, respectively.

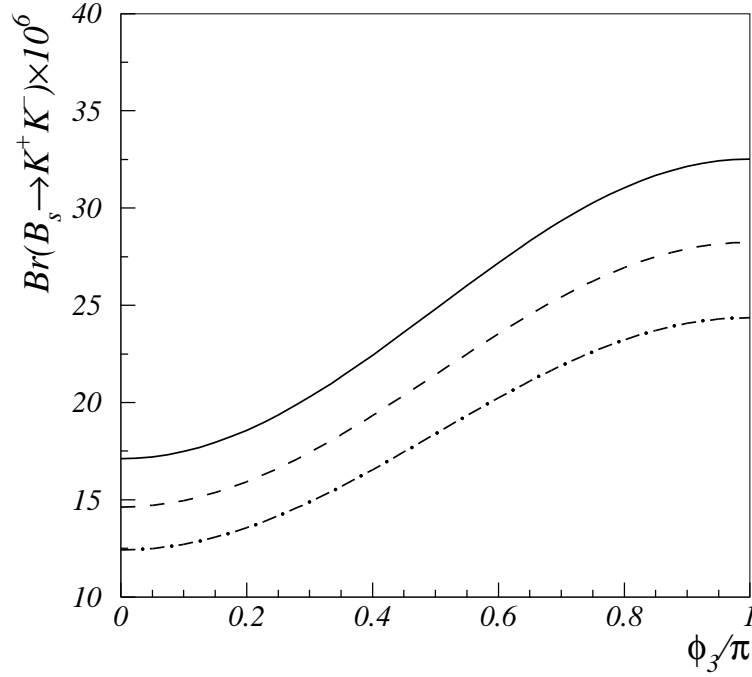


Figure 3: The CP average BR of  $B_s \rightarrow K^+ K^-$  as a function of  $\phi_3$  with  $\omega_B = 0.4$  GeV. The solid, dashed and dashed-dot lines denote  $m_K^0 = 1.7, 1.6$  and  $1.5$  GeV, respectively.

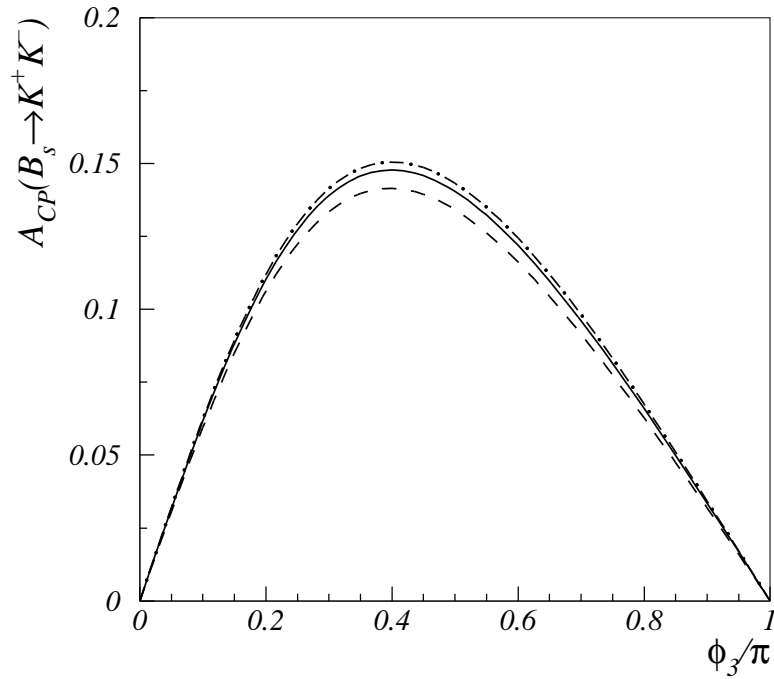


Figure 4: The CP asymmetry of  $B_s \rightarrow K^+ K^-$  with  $m_K^0 = 1.7$  GeV. The dashed, solid and dashed-dot lines represent  $\omega_B = 0.41, 0.4$  and  $0.38$  GeV, respectively.